internal report 293

Sediment characteristics and concentration gradients in the RP1 constructed wetland filter

D Klessa
C Hunt
C leGras

July 1998

supervising scientist

Sediment characteristics and concentration gradients in the RP1 constructed wetland filter

David Klessa, Craig Hunt and Chris leGras

Abstract

Key words: sediment chemistry, constructed wetland filter, total uranium, labile uranium, speciation, total manganese, total cobalt.

The compartmentalisation of contaminants, derived from restricted release zone water, into sediment of the Retention Pond #1 Constructed Wetland Filter (RP1 CWF) at Ranger was studied. Following two seasons during which RP2 water was processed by the RP1 CWF, sediment was sampled from the 0–1, 1–3, 3–5 and 5–10 cm depths of the cells. Sediment samples were assayed for pH, electrical conductivity, cation exchange capacity (CEC), exchangeable bases, available P and total N, P, C, U, Cu, Cd, Pb, Co, Zn, Mn and Fe. Sodium bicarbonate (0.5 M) buffered at pH 8.5 was also used to extract a labile uranium fraction from sediment.

Sediment was characterised by a moderate to slightly acid pH (4.6–6.5), very low to moderate CEC (0.4–11.3 $\mathrm{cmol_+/kg}$) and low organic C content (0.6–1.6%). Total U concentration decreased in an approximately exponential fashion with path length and depth from a maximum of 570 mg/kg in Cell 1 surface sediment. On average, 51% of total U was extracted by bicarbonate. It was estimated that around 64–77% of the retained U load from the polishing of RP2 water could be accounted for in the sediment of the wetland filter.

The speciation of U in influent water to the RP1 CWF is discussed. The more acid pH and CO_2 enriched environment of sediment pore water compared to the overlying water column will favour the speciation and sorption of the mononuclear cation and hemicarbonate forms of U which are preferentially adsorbed by oxyhydroxide surfaces. Total U was highly correlated with total Mn which might imply the active sequestering of U by Mn oxide surfaces. A similarly high correlation was found between total Mn and Co which was attributed largely to native soil minerals. However, the relative enrichment of surface sediment by Mn and Co, especially in the front cells, suggests that the formation of Mn oxides and the sorption of Co is an active process.

1 Introduction

1.1 Background

The Retention Pond 1 Constructed Wetland Filter (RP1 CWF), situated to the east of the RP1 catchment, comprises eight cells of varying size with a combined surface area of approximately 5.8 ha, flow path length 1.08 km, total volume 49637 m^3 and a maximum water depth within the flow path of 0.5–1.6 m (Table 1.1). First commissioned in 1995 to polish RP2 water, the RP1 CWF (Fig 1) combined two existing experimental wetland filters, each composed of three relatively small cells (Nisbet 1995), by interconnection with three new, relatively large, cells occupied formerly by a borrow pit (ERA 1996b).

Table 1.1 Dimensions of the RP1 CWF

Cell	Flow path length (m)	Surface area (m^2)	Maximum depth range (m)
1	53 (122†)	1890	0.6–1.2
2	30 (116†)	1880	0.9–1.4
3	31	1450	1.0–1.2
4	324	18700	0.7–1.0
5	67	2290	0.5–1.1
6	159	7150	1.1–1.6
7	221	15000	0.5–0.7
8	200	10400	0.7–0.8
Total	**1085**	**58760**	

†In 1995, path length was increased by the installation of plastic barrier to provide an estimated length shown in parenthesis

1.2 Performance in 1995

During its first year of operation, the RP1 CWF treated 450 800 m^3 of RP2 water with 283 700 m^3 applied to the RP1 flood irrigation area water (ERA 1996b). Input and output loads for 1995 are given in Table 1.2. The efficacy by which uranium (U) was polished decreased almost linearly over the first two months from near 100% to 50% and then increased over the remaining two months to 60% (ERA 1996). Overall, this removal of U has been estimated, by accounting for the retention time of solute 'pulses', at around 50% (ERA 1996) and 54% (leGras & Klessa 1997), or by corrected mass balance (Table 1.2) at 55%. Similarly, manganese (Mn) attenuation was found to be 96% (leGras & Klessa 1997) and 91% (Table 1.2). Sulphate (SO_4) and magnesium (Mg) behave conservatively and there is no evidence to suggest that the rate of reduction of sulphate favours its net removal in the RP1 CWF (ERA 1996, leGras & Klessa 1997). Because of their conservative properties, either Mg or SO_4 can be used in ratio to U at inlet and outlet as a signature to follow sorption and transport processes through the wetland filter.

Changes in the SO_4:U ratios for entry into and exit from each cell of the RP1 CWF during 1995 are shown in Figure 1.2 derived from ERA data (ERA 1996a). These data were used to calculate the mean efficiency of each cell (Table 1.3) to polish U over the 1995 season. Over half of the U retained within the whole of the RP1 CWF was removed by just two cells, namely Cells 4 and 7 which, combined, make up 50% of the total path length and 57% of the total surface area (Table 1.1). However, when efficiency is expressed on either a standard length, area or volume basis, the most efficient cells were the maturest ones in terms of

Table 1.2 Input and output loads to and from the RP1 CWF during the 1995 dry season. Corrected values are shown in italics (see text).

	U (kg)		Mn (kg)		Fe (kg)		SO_4 (t)	Mg (t)
	<0.4 µm	>0.4 µm	<0.4 µm	>0.4 µm	<0.4 µm	>0.4 µm		
Input (a)	367.1	6.1	125.3	23.6	9.8	45.6	215.3	51.8
[1]Output (b)	103.6	0.6	1.5	0.7	6.6	24.9	135.8	33.3
	(140.6)	*(0.8)*	*(2.0)*	*(1.0)*	*(9.0)*	*(33.8)*	*(184.3)*	*(45.1)*
[2]Residue (c)	25.2	0.3	10.4	0.4	2.8	9.7	30.9	7.2
b+c	128.8	0.9	11.9	1.1	9.4	34.6	166.7	40.5
	(165.8)	*(1.1)*	*(12.4)*	*(1.4)*	*(11.8)*	*(43.5)*	*(215.2)*	*(52.3)*
a-(b+c)	243.5		135.9		11.4		48.6	11.3
	(206.3)		*(135.1)*		*(0.1)*		*(0.1)*	*(-0.5)*
% retained	65.2		91.3		20.6		22.6	21.8
	(55.3)		*(90.7)*		*(0.2)*		*(0)*	*(-1.0)*

[1] Calculated using mean weekly flow (Fig 7, ERA 1996) to RP1 flood irrigation area between weeks ending 26/7/95 and 1/11/95.

[2] Represents load associated with residual RRZ water in the CWF at the termination of flow on 1/11/95; calculated from surface area and mean depth of cells (Table 1.1) and concentration (ERA 1996) in cell waters on 8/11/95

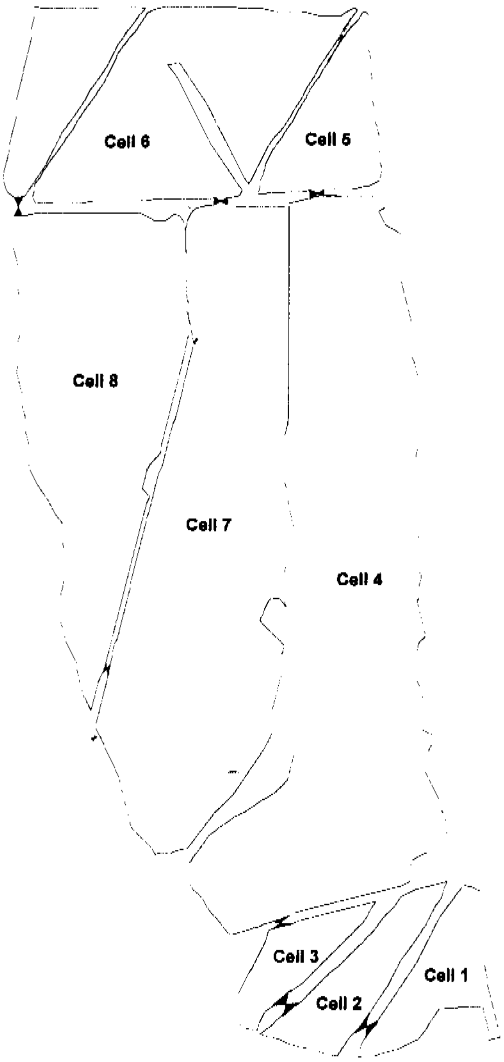

Fig 1.1 Layout of the RP1 CWF

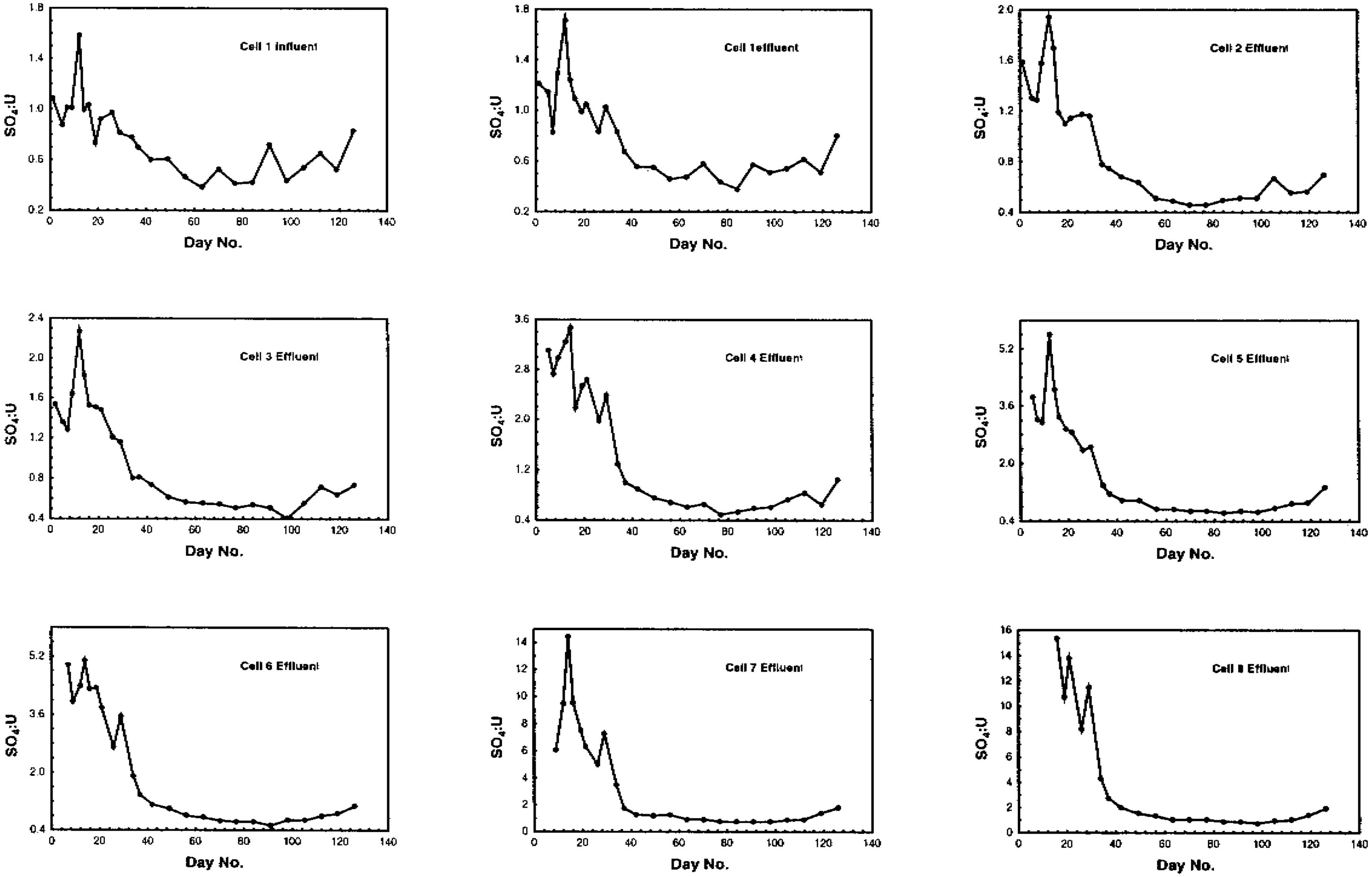

Fig 1.2 SO$_4$:U ratios in the RP1 CWF (1995)

Table 1.3 Efficiency of U removal (% of total load) during 1995 by each cell in the RP1 CWF

	Cell							
Efficiency	**1**	**2**	**3**	**4**	**5**	**6**	**7**	**8**
Mean efficiency (%)	1.5	6.7	5.2	17.9	9.9	-1.3	15.0	3.4
Efficiency/km	28.5	222.9	166.5	55.4	147.1	-	68.0	16.6
Efficiency/ha	8.0	35.6	35.6	9.6	43.0	-	10.0	3.2
Efficiency/1000 m^3	0.9	3.1	3.2	1.1	5.4	-	1.7	0.4

plant biomass production. On average, Cells 2, 3 and 5 were around 3 times more efficient than the remainder of the CWF (Table 1.3) at removing U. The negative efficiency (ie net release of U) of Cell 6 may simply point to a problem of representative sampling of Cell 5 effluent/Cell 6 influent since exchange between cells occurs by pipe subflow compared to surface flow elsewhere.

The apparent 'unaccounted for' SO_4 and Mg which shows up in a mass balance (Table 1.2) most probably reflects inaccuracies in the monitoring of the volume of treated RP 2 which was flood irrigated. For example, the difference of 167 100 m^3 (see above) between input and output volumes in 1995 cannot all be attributed to evapotranspiration. If 1 m evapotranspiration from the RP1 CWF is assumed over the processing period, this equates to a loss of approximately 59 000 m^3. In turn, this suggests that 'output' (Table 1.2) may be underestimated by about a factor of about 38/28 (ie 1.36). If data is adjusted to take account of this factor (see italics), both SO_4 and Mg appear conservative and there is excellent agreement between values for the attenuation of U quoted here and elsewhere.

1.3 Performance in 1996

In 1996, input of RP2 water amounted to 164 400 m^3 and output to flood irrigation was 83 500 m^3 (ERA 1997). The pattern to the efficacy of U removal appeared similar to that shown in 1995 with U concentration falling from 90% initially (*vis à vis* input versus output concentration) to a minimum of around 50% by the end of the process period (ERA 1997).

Estimates of U removal efficiency in 1996 range from 78% (leGras & Klessa 1997) and 81% (ERA 1997) by accounting for retention time, and 92% by mass balance (ERA 1997). Our estimate of U retention by mass balance is around 73% (Table 1.4) and 78% for Mn using the same correction factor as for the 1995 data. It is important to note, however, that the lack of time series data for each cell prevents either a meaningful comparison to be made of cell efficiencies or a rigorous analysis of overall efficiency, especially relative efficiency compared to 1995. Since a much lower volume of water passed through the RP1 CWF in 1996 compared to 1995, resulting in longer retention times approximating to 1.5 cell volume (leGras & Klessa 1997), performance is, not surprisingly, higher in 1996. As with the 1995 data, the 1996 output volume to flood irrigation (ERA 1997) is probably underestimated which, in turn, tends to exaggerate the efficiency of the RP1 CWF and underestimates loadings to the RP1 flood irrigation area.

Table 1.4 Input and output loads to and from the RP1 CWF during the 1996 dry season. Corrected values are shown in italics (see text).

	U (kg)		Mn (kg)		Fe (kg)		SO_4 (t)	Mg (t)
	<0.4 µm	>0.4 µm	<0.4 µm	>0.4 µm	<0.4 µm	>0.4 µm		
Input (a)	64.5	2.0	19.8	1.5	7.6	32.2	67.6	16.7
[1]Output (b)	3.8 *(5.2)*	0.1 *(0.1)*	1.4 *(1.9)*	0.7 *(1.0)*	3.3 *(4.5)*	11.4 *(15.5)*	26.7 *(36.3)*	7.1 *(9.7)*
[2]Residue (c)	12.3	0.2	1.3	0.4	1.4	7.9	25.8	6.6
b+c	16.1 *(17.5)*	0.3 *(0.3)*	2.7 *(3.2)*	1.1 *(1.4)*	4.7 *(5.9)*	19.3 *(23.4)*	52.5 *(62.1)*	13.7 *(16.3)*
a-(b+c)	50.1 *(48.7)*		17.5 *(16.7)*		15.8 *(10.5)*		15.1 *(5.5)*	3.0 *(0.4)*
% retained	75.3 *(73.2)*		82.2 *(78.4)*		39.7 *(26.4)*		22.3 *(8.1)*	18.0 *(2.4)*

[1] Calculated using daily flow to the RP1 flood irrigation area until week ending 2/9/96; data (in italics) represents corrected mass using a factor of 1.36.

[2] Represents load associated with residual RRZ water in the CWF at the termination of influent flow.

1.4 Objectives of this study

In the report which follows, the chemical properties of *sediment* sampled from the RP1CWF are described and discussed. The word *sediment* has been italicised to draw attention to the fact that strictly speaking the substrate sampled bears more resemblance and has properties more akin to (weakly hydromorphic) soil than sediment. This is because the wetland system is immature. Much of the land area upon which the RP1 CWF is situated, and the soil used to engineer the wetland, only became permanently inundated recently during the 1995 dry season. Edaphically, the system is in disequilibrium. In addition, processes that give rise to the formation of sediment, particularly involving C cycling, are in the early stages of evolving. Given these restrictions to the meaning attached to *sediment* in the context of the RP1 CWF, we have used the word liberally throughout this report.

The objectives were as follows;

1. to determine (path length and depth) concentration gradients in RP1 CWF sediment of components of RRZ water.
2. to examine the chemical properties of sediments in the RP1 CWF.
3. to relate the chemical characteristics of sediment in the RP1 CWF to performance criteria.

2. Methods

2.1 Sediment sampling and preparation

Sediment samples from the RP1 CWF were collected in February 1997 from each of the cells with the exception of Cell 6. A stainless steel piston corer (37 mm ID) was driven into the sediment from a moored boat and on extraction of intact cores, sediment was divided into 0–10, 10–30, 30–50 and 50-100 mm depth segments, and then bagged. Representative samples were obtained from Cells 1, 2, 3 and 5 (Fig 1.1) by sampling within the flow path, near the inlet, outlet and from the middle of each cell, and combining to form a composite sample. Cells 4, 7 and 8, which have longer flow paths (Table 1.1), were sampled by obtaining separate samples from the inlet, middle and outlet regions of each of these cells. Generally, each representative sample was composed of 20 cores and taken within the vicinity of plant growth, principally *Eleocharis sphacelata* which dominates the RP1 CWF. Cell 6 was not sampled because of access difficulty to the sediment by virtue of deep water in the flow path.

Prior to analyses, samples were air-dried at 35 °C and then passed through a 5 mm sieve to remove stones and coarse gravel which were discarded. The <5 mm fraction was then ground using an agate mortar and pestle to pass through a 2 mm sieve. For some analyses (indicated below), representative subsamples of each sediment sample were ground to <0.15 mm.

2.2 Analyses

With the exception of total P and microwave digestion for total metals, all analyses followed published and/or in-house methods (Table 2.1). Sample runs always incorporated a quality assurance protocol by including reference materials and blanks in the assays. Concentration was always corrected to account for the air-dry moisture content of sediment samples. In most sample runs, a minimum of one sediment sample was replicated at least three times to account for within-sediment sample variation.

Table 2.1 Methods employed in sediment sample analyses

Assay	Method	Method Reference[1]
Air-dry (AD) moisture	105 °C to constant weight	2A1
pH	1:5 soil:water suspension	4A1
Electrical conductivity	1:5 soil:water suspension	3A1
Cation exchange capacity	0.01 M silver thiourea ($AgTU^+$)	15F3
Exchangeable bases	0.01 M silver thiourea ($AgTU^+$)	15F1
Total organic carbon[5]	Heanes wet oxidation	6B1
Total nitrogen[5]	Kjeldahl acid digestion	ARRRI 611
	Indophenol blue	7A2[2]
Extractable phosphorus	Olsen extractable; 1: 20 extract	9C1
Total phosphorus[5]	Acid persulphate digestion	See footnote[3]
Total metals (Cd, Co, Cu, Fe, Mn, Pb, U, Zn)[5]	Microwave *aqua regia* digestion	In-house[4]
	ICPMS, ICPAES	
Extractable uranium	Olsen extractable; 1: 20 extract	In-house[4]

[1] Rayment & Higginson (1992); [2] Translation of automated into manual method; [3] Adapted from Fuller (1997); [4] Methods currently being developed; [5] Conducted on <0.15 mm sediment.

Total P in sediment was determined by modifying a method given by Fuller (1997) involving the use of persulphate as an oxidising agent under strongly acidic conditions. A known mass of sediment, approximately 0.250 g, was placed in a 50 ml screw-topped tube, capable of being autoclaved, to which 5 ml deionised water, 5 ml 5.5M H_2SO_4 and 2.0 g potassium persulphate ($K_2S_2O_8$) were added. The tube was then stoppered and placed in an autoclave for 1 h. After time to cool and settle, a 0.5 mL aliquot was placed in a 25 mL volumetric flask and 5 mL deionised water added. One drop of phenolphthalein indicator was dispensed into the flask and the contents neutralised (faint pink) using approximately 4 M NaOH, followed by 4 mL of mixed reagent[1]. The volume was then made up to the mark with deionised water. Absorbance was read in 1 cm cells at 882 nm using deionised water as a reference. Standards were prepared initially by diluting 0, 200, 400, 600, 800, 1000, 1500 and 2000 µL of a 100 µg/mL P standard in 100 mL volumetric flasks each containing 50 mL 5.5 M H_2SO_4 and made up to the mark with deionised water. A 5 mL aliquot of each standard was then placed in 25 mL volumetric flasks to provide 0, 0.04, 0.08, 0.12, 0.16, 0.20, 0.25 and 0.30 µg/mL H_2PO_4-P and the same procedure followed as described above for samples. The discrepancy between the proportion of NaOH to total volume (ie 25 mL) used to neutralise acid in the samples compared to the standards was not important (in relation to a source of orthophosphate contamination) since the blank standard always provided zero absorbance.

Microwave digestion for total metals was conducted using approximately 0.500 g sediment and 10 mL HNO_3 and involved a 5 minute 30 seconds ramp to and 4 minute 30 seconds dwell at 175 °C with a power input of 1000 W. After cooling, samples were diluted with deionised water to provide 1% HNO_3 solutions for analysis by ICPMS and ICPAES.

3. Results

A compendium of results is contained in the Appendix.

3.1 pH and conductivity

pH and conductivity over the whole wetland filter and for all sampling depths ranged between 4.6–6.5 and 22-266 µS/cm respectively with Cell 3 sediment having the lowest pH and highest conductivity. In general, pH increased and conductivity decreased with depth (Table 3.1) but there are no discernible gradients along the length of the CWF (Table 3.2).

Table 3.1 Mean pH and conductivity of sediment at each sampling depth

		Depth (cm)			
		0–1	1–3	3–5	5–10
pH	mean	5.55	5.76	5.84	5.78
	SD	0.51	0.40	0.27	0.40
EC (µS/cm)	mean	128	63	59	65
	SD	55	35	19	25

---

[1] Mixed reagent is composed by preparing and mixing 'reagent A' and 'reagent B', details of which can be found in Rayment & Higginson (1992), p 69.

Table 3.2 Sediment pH and conductivity in the 0–1 and 0–10 cm sediment depths of each cell

		Cell						
	Depth (cm)	**1**	**2**	**3**	**4†**	**5**	**7†**	**8†**
pH	0–1	5.29	6.27	4.81	6.08	5.03	5.34	5.47
	0–10	5.96	6.33	5.79	5.81	5.47	5.65	5.69
EC (µS/cm)	0–1	126	158	266	79	176	117	117
	0–10	57	91	102	54	66	69	73

†Mean of inlet, middle and outlet.

3.2 Cation exchange capacity and exchangeable bases

Cation exchange capacity (CEC) ranged between 0.4–11.3 cmol_+/kg with the highest values associated with relatively clay rich substrate (eg Cell 8 inlet) and the lowest with subsurface sandy material (eg Cell 2 & Cell 4 inlet). In general, the 0–1 cm surface sediment displayed the highest CEC within the sampled profile (Table 3.4) but CEC did not vary markedly between cells (Table 3.5).

Magnesium (Mg^{2+}) dominates the exchange sites (Tables 3.4 & 3.5), comprising an average of 78% of total exchangeable bases. This figure, together with data for exchangeable Mg^{2+} contained in Tables 3.4 & 3.5, is derived by correcting for a small quantity of soluble salt which was present in the sediment samples (see electrical conductivity data above) and which was not removed prior to undertaking analyses of exchangeable bases and CEC. Where CEC is low, the presence of small quantities of soluble salt can give rise to a significant error which becomes especially obvious when reconciling total exchangeable bases with CEC. The correction was made by first translating measured electrical conductivity to ionic strength using the Marion-Babcock equation *viz*

$$\log I = 1.159 + 1.009 \log EC \quad (r^2 = 0.994;\ SD = \pm 0.049 \text{ log units})$$

where I = ionic strength (mmol/L)

EC = electrical conductivity (dS/m) within the range 0–16 dS/cm.

The ionic strength of the 1: 5 soil extraction was then assumed to derive solely from $MgSO_4$ allowing the contribution of free Mg^{2+} to be calculated as cmol_+/kg (Fig 3.1) and a correction to exchangeable Mg to be made.

The relative abundance of exchangeable bases is in the order $Mg^{2+} >> Ca^{2+} > K^+ \geq Na^+$ and reflects the composition of RP2 water passing through the CWF. Mean base saturation for the 0–10 cm depth ranges between 42–73% (Table 3.4) which is to be expected given the slightly- to moderately-acidic pH of the sediments (Table 3.2).

3.3 Total organic carbon and total nitrogen

Surface (0–1 cm) sediment throughout the RP1CWF is low in organic C ranging between 0.57–1.61% which equates to an organic matter content[2] of approximately 1.0–2.8%. Generally, organic C declines with depth (Table 3.5 & 3.6) and is higher in surface (0–1 cm) sediment from the older cells (ie. Cells 1, 2 & 5). However, the newer cells (especially Cells 7 & 8) contain more organic C at depth than the more mature cells and this may be due to

---

[2] Assuming a conversion factor of 1.724 (Hesse 1971).

Table 3.4 Mean CEC of sediment and exchangeable bases at each sampling depth

		Depth (cm)			
(cmol$_+$/kg)		**0–1**	**1–3**	**3–5**	**5–10**
CEC	mean	4.78	3.59	3.71	3.90
	SD	2.48	1.55	2.03	1.91
Mg†	mean	1.99	1.60	1.88	1.99
	SD	0.81	0.54	1.09	1.36
Ca	mean	0.48	0.30	0.29	0.39
	SD	0.22	0.11	0.13	0.17
K	mean	0.11	0.06	0.07	0.08
	SD	0.05	0.03	0.04	0.07
Base saturation (%)	mean	63.8	69.3	76.8	71.4
	SD	35.2	52.7	60.1	36.2

†Mg adjusted to take account of soluble salts (see text).

Table 3.4 CEC and exchangeable bases in the 0–1 and 0–10 cm sediment depths of each cell

		Cell						
(cmol$_+$/kg)	**Depth (cm)**	1	2	3	4†	5	7†	8†
CEC	0–1	5.74	5.93	5.80	2.42	1.81	4.53	7.66
	0–10	5.38	2.32	4.29	2.79	2.39	4.62	5.24
Mg††	0–1	2.60	2.20	1.37	1.46	1.62	1.81	2.76
	0–10	1.72	1.85	1.68	1.34	1.13	2.84	1.88
Ca	0–1	0.71	0.66	0.46	0.32	0.26	0.42	0.64
	0–10	0.43	0.43	0.37	0.31	0.27	0.44	0.33
K	0–1	0.09	0.09	0.07	0.10	0.08	0.11	0.13
	0–10	0.07	0.07	0.05	0.10	0.06	0.10	0.05
Na	0–1	0.08	0.03	0.02	0.05	0.05	0.04	0.05
	0–10	0.03	0.03	0.03	0.03	0.06	0.04	0.02
BS (%)	0–1	60.6	50.2	33.3	*93.1*	*111.3*	52.9	45.1
	0–10	41.7	*102.6*	49.5	72.6	63.8	73.3	43.4

†Mean of inlet, middle and outlet;††Mg adjusted to take account of soluble salts (see text).

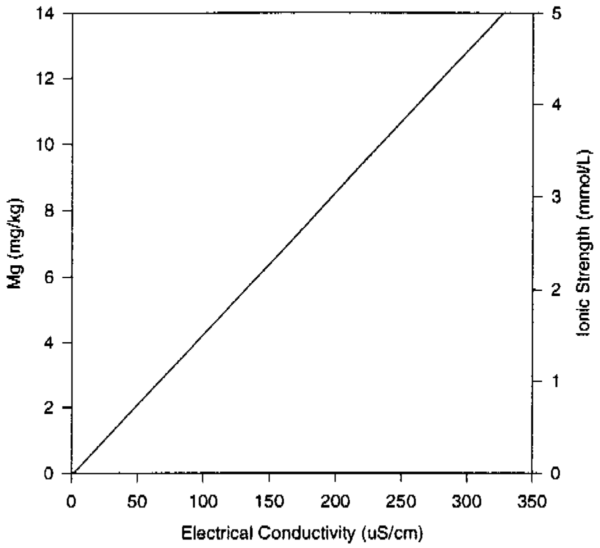

Fig 3.1 Estimated Mg concentration in soil solution from EC determination of sediments using the Marion-Babcock equation and assuming $MgSO_4$ to be the dominant salt.

landscaping with topsoil during engineering works and the dumping of organic matter in the CWF from bush clearing operations in preparation to mining orebody #3. The distribution of total N largely matches that of total organic C (Tables 3.5 & 3.6). Total N in surface (0–1 cm) sediment ranges between 0.03–0.12% and declines with depth. C:N ratios in the surface (0–1 cm) indicate that the organic matter it contains is partially humified. The increase in C:N ratio down the profile (Table 3.6) is in contrast to the trend normally seen in sedentary soil and may reflect the predominance of fresh roots over that of humified material at depth in these young sediments.

Table 3.5 Mean total organic C and total N contents, and C:N ratios of sediment at each sampling depth

		Depth (cm)			
		0–1	1–3	3–5	5–10
Total C (%)	mean	1.08	0.66	0.63	0.56
	SD	0.35	0.16	0.12	0.18
Total N (%)	mean	0.056	0.021	0.018	0.012
	SD	0.027	0.010	0.010	0.008
C:N ratio		19.3	31.4	35.0	46.7

Table 3.6 Total organic C and total N contents and C:N ratios in the 0–1 and 0–10 cm sediment depths of each cell

	Depth (cm)	Cell 1	2	3	4†	5	7†	8†
Total C (%)	0–1	1.61	1.09	0.89	0.72	1.45	1.05	1.23
	0–10	0.59	0.54	0.46	0.50	0.71	0.74	0.78
Total N(%)	0–1	0.121	0.070	0.047	0.036	0.099	0.045	0.049
	0–10	0.031	0.023	0.008	0.022	0.033	0.010	0.022
C:N ratio	0–1	13.3	15.6	18.9	20.0	14.6	23.3	25.1
	0–10	19.0	23.5	57.5	22.7	21.5	74.0	35.4

3.4 Total and available phosphorus

Total P is very low in RP1 CWF sediment, commonly <0.02%, and declines with depth (Table 3.7). The highest total P concentration for both surface (0–1 cm) and 'whole' sediment (ie 0–10 cm) is found in Cells 1 and 2 (Table 3.8). Total N:P ratios at the 0–1 cm depth range from 2.1–7.1. Available P constitutes <2% of total P and also declines with depth.

Table 3.7 Mean total and available P contents, and total N:P ratios of sediment at each sampling depth

		Depth (cm) 0–1	1–3	3–5	5–10
Total P (%)	mean	0.017	0.014	0.013	0.012
	SD	0.007	0.004	0.005	0.003
Available P (mg/kg)	mean	1.64	1.46	1.28	1.21
	SD	0.50	0.37	0.20	0.23
Total N:P ratio		3.3	1.5	1.4	1.0

Table 3.8 Total and available P contents and total N:P ratios in the 0–1 and 0–10 cm sediment depths of each cell

	Depth (cm)	Cell 1	2	3	4†	5	7†	8†
Total P (%)	0–1	0.028	0.034	0.020	0.012	0.014	0.013	0.016
	0–10	0.020	0.020	0.018	0.010	0.010	0.012	0.012
Available P (mg/kg)	0–1	1.56	2.46	1.81	1.58	2.62	1.52	1.17
	0–10	0.91	1.32	1.15	1.38	1.68	1.28	1.37
Total N:P ratio	0–1	4.3	2.1	2.4	3.0	7.1	3.5	3.1
	0–10	1.6	1.2	0.4	2.2	3.3	0.8	1.8

3.5 Total cadmium, cobalt, copper, iron, manganese, lead and zinc

In general, and with the exception of Fe, metal concentrations are highest in surface (0–1 cm) sediment and decline with depth (Table 3.9). The most well-defined concentration gradients along path length are shown by Co and Mn (Tables 3.10 & 3.11) but the presence of 'hot spots' of Cd, Pb and Zn in Cells 5, 7 and 8 sediments (Appendix 1) confound evidence of path length gradients for these metals. These 'hot spots' may derive from pyritic minerals contained in crushed non-mineralised waste rock used as bottoming in the construction of the filter (P Wood, pers comm).

Table 3.9 Mean total Cd, Co, Cu, Fe (%), Mn, Pb and Zn contents (mg/kg) of sediment at each sampling depth

		Depth (cm)			
mg/kg		**0–1**	**1–3**	**3–5**	**5–10**
Cd	mean	0.673	0.298	0.039	0.026
	SD	1.726	0.509	0.032	0.022
Co	mean	4.23	2.73	2.71	2.27
	SD	3.57	1.79	1.73	1.25
Cu	mean	19.67	16.38	14.78	15.68
	SD	9.72	10.81	6.97	6.88
Fe (%)	mean	2.24	1.97	2.19	2.31
	SD	0.84	0.79	1.05	1.11
Mn	mean	82.45	38.81	33.89	25.50
	SD	68.46	30.92	25.13	15.16
Pb	mean	14.56	10.73	10.31	10.93
	SD	10.48	4.02	3.43	3.39
Zn	mean	88.93	34.68	13.78	9.28
	SD	189.86	54.23	11.32	4.92

Table 3.10 Total Cd, Co, Cu, Fe (%), Mn, Pb and Zn contents (mg/kg) in the 0–1 and 0–10 cm sediment depths of each cell

		Cell						
	Depth (cm)	**1**	**2**	**3**	**4†**	**5**	**7†**	**8†**
Cd	0–1	0.058	0.042	0.033	0.023	6.565	0.195	0.465
	0–10	0.014	0.016	0.058	0.014	1.093	0.089	0.143
Co	0–1	14.17	9.22	5.58	1.70	2.39	2.78	3.41
	0–10	5.65	4.02	3.20	1.36	1.64	3.05	2.23
Cu	0–1	37.18	39.09	17.28	11.49	18.90	15.83	20.44
	0–10	17.74	18.99	12.46	12.21	10.13	19.89	17.64
Fe (%)	0–1	3.03	2.11	1.61	1.84	1.32	2.35	2.83
	0–10	1.58	1.95	2.15	1.85	1.04	2.95	2.55
Mn	0–1	251.48	207.38	85.26	54.60	34.46	55.16	24.72
	0–10	62.72	83.24	39.81	16.87	16.35	40.33	29.41
Pb	0–1	13.94	8.38	6.52	10.11	47.92	11.92	15.50
	0–10	6.88	8.53	9.22	9.75	13.95	12.75	12.87
Zn	0–1	47.56	31.18	19.86	12.25	734.96	29.55	65.70
	0–10	18.87	12.99	29.03	8.71	123.70	11.47	18.92

Table 3.11 Correlation of sediment total metal concentrations and extractable U with path length for a given sediment depth (n = 13). Significance is shown at the p<0.05, 0.01 and 0.001 levels.

	Depth (cm)			
Metal	**0–1**	**1–3**	**3–5**	**5–10**
Cd	0.033	0.157	0.400	0.354
Co	-0.485	-0.383	-0.260	0.133
Cu	-0.282	0.180	0.221	0.429
Fe	0.319	0.358	0.446	0.474
Mn	-0.585*	-0.348	-0.239	0.236
Pb	0.132	0.377	0.630*	0.644**
U	-0.571*	-0.482	-0.565*	-0.586*
Extractable U	-0.574*	-0.498	-0.555*	-0.533
Zn	0.007	0.046	-0.464	-0.537

Table 3.12 Correlation matrix between total metal, extractable U and total organic C concentrations, and CEC (n = 52). Significance is shown at the p<0.05, 0.01 and 0.001 levels.

	Tot. Co	**Tot. Cu**	**Tot. Zn**	**Tot. Cd**	**Tot. Pb**	**Tot. U**	**Tot. Mn**	**Tot. Fe**	**Org. C**	**Ex. U**
Tot. Cu	0.716***									
Tot. Zn	0.015	0.093								
Tot. Cd	-0.061	0.035	0.992***							
Tot. Pb	0.017	0.282*	0.870***	0.868***						
Tot. U	0.822***	0.534***	0.268	0.203	0.182					
Tot. Mn	0.910***	0.691***	0.021	-0.052	0.028	0.883***				
Tot. Fe	0.270	0.599***	-0.080	-0.099	0.379**	0.068	0.229			
Org. C	0.476***	0.458***	0.401**	0.366**	0.455***	0.617***	0.527***	0.200		
Ex. U	0.702***	0.506***	0.356**	0.299*	0.231	0.928***	0.781***	0.019	0.594***	
CEC	0.292*	0.264	-0.039	-0.051	0.117	0.241	0.227	0.360**	0.330*	0.245

There is high correspondence between total Co and Cu, Co and Mn, Cu and Mn, and Cu and Fe in sediment (Table 3.12). When data is normalised by taking logarithms, significant ($p<0.001$) relationships are shown (Fig 3.2). The same metals are also positively correlated with organic matter. The removal of Cd, Pb and Zn data outliers to normalise these data sets neither established significant ($p<0.05$) relationships between these metals concentrations and organic matter content, nor path length.

Stepwise regression was conducted on metal concentrations to establish best-fit relationships. In the cases of Co, Cu, Mn and Fe as dependent variables, the full data set (ie n = 52) was used. However, when Zn, Cd and Pb were dependent variables, outliers were first removed (ie n =46). Results of multiple regression are summarised in Table 3.13.

Several key variables emerge as predictors of total (logged) metal concentrations in sediment. When Pb, Cu or Mn are dependent variables, the Fe and Co contents of sediment are important predictors. With the exception of the inverse relationship between Pb and Co, metal concentrations are positively related to Fe and Co concentrations in sediment.

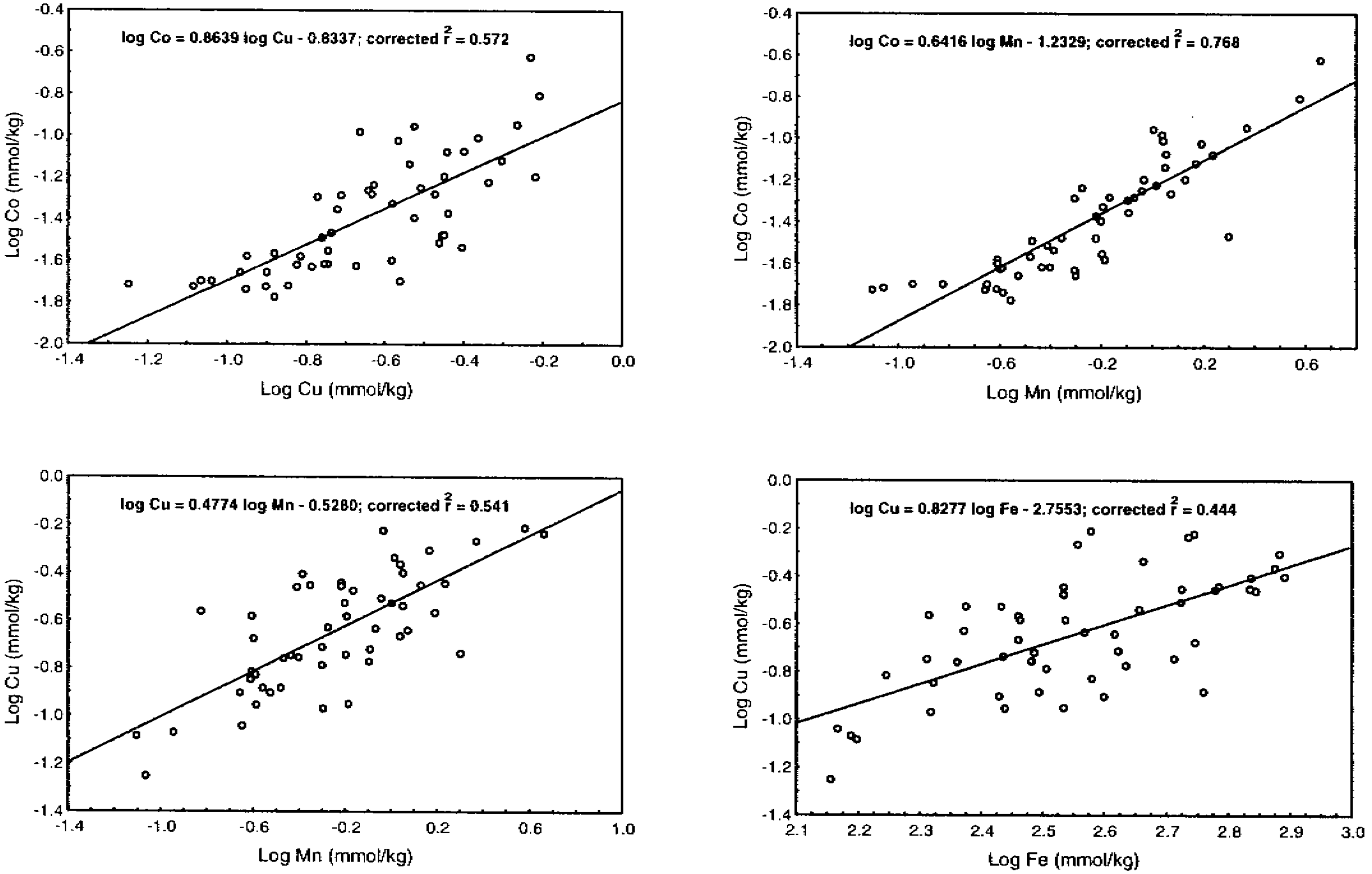

Fig 3.2 Relationships ($p<0.001$) between (logged) total Co, Cu, Fe and Mn in sediment ($n = 52$)

Table 3.13 Derived best-fit regression relationships for total metals and extractable U in sediment

				Independent variable								
Dep. variable	**s_y**	**corrected r^2**	**Constant**	**log Co**	**log U**	**log Fe**	**log Zn**	**log Mn**	**log org C**	**path length**	**mean depth**	**CEC**
log Zn	0.2264	0.441***	-0.4174	–	0.3683***	–	–	–	–	–	–	–
log Cd	0.3142	0.601***	-3.8531	–	–	–	0.5844**	–	-1.3932**	7.981e-4***	-0.0946***	0.1007**
log Pb	0.0439	0.878***	-3.2504	-0.1697***	–	0.6749***	–	–	0.1443**	–	–	–
log Cu	0.1297	0.720***	-1.2754	0.5116***	–	0.5264***	–	–	–	–	–	–
log Mn	0.1473	0.850***	0.1141	0.8080***	0.2314***	0.3752**	–	–	–	–	–	–
log Co	0.1299	0.782***	-1.2758	–	–	–	–	0.6839***	–	–	0.0153*	–
log Fe	0.1352	0.542***	2.3770	–	–	–	–	0.4064***	-0.5022***	3.5733e-4***	–	–
log U	0.2977	0.709***	-0.1556	–	–	–	–	0.7594***	–	-3.3260e-4**	-0.0909***	–
log ex. U	0.3426	0.730***	-0.3480	–	-	–	–	0.8266***	–	-3.9250e-4**	-0.1142***	–

1. Significance at the $p = 0.05$, 0.01 and 0.001 levels is shown by asterisks.
2. Units of concentration are mmol/kg except for CEC (cmol$_c$/kg) and organic C (%).
3. Units of path length and mean depth are m and cm respectively.
4. s_y is the standard deviation of the dependent variable.

Cobalt and Fe concentrations are directly proportional to Mn content, and organic matter content is a predictor of sediment Pb, Cd and Fe concentrations. While Pb is positively related to organic matter content, Cd and Fe are inversely related. This apparent similarity between Fe and Cd in concentration distribution is also shown by their sharing of path length as a predictor with an increase in concentration through the RP1 CWF as a function of distance (ie when holding other factors constant). While Cd concentration decreases with sediment depth, Co concentration shows a slight increase. The concentrations of both Zn and Mn are positively related to U concentration and Cd is proportional to CEC.

3.6 Total and bicarbonate-extractable uranium

Strong concentration gradients of U are found in the sediments of the RP1 CWF both in the direction of flow and with depth (Tables 3.14 & 3.15). This decline in U concentration with sediment depth and distance from the inlet of Cell 1 is approximately exponential (Fig 3.4). For example, in surface (0–1 cm) sediment, U fell from a maximum of about 0.06% in Cell 1 to a minimum in Cell 7 of an order of magnitude less (Appendix 1).

Table 3.14 Mean total U and extractable U contents of sediment at each sampling depth

		Depth (cm)			
		0–1	1–3	3–5	5–10
Total U (mg/kg)	mean	189.9	62.1	35.8	16.5
	SD	148.6	64.6	44.7	12.4
Extractable U (mg/kg)	mean	113.7	37.2	16.9	7.8
	SD	82.0	43.4	23.5	7.2
Extractable U (% of total)	mean	61.1	58.2	41.8	42.5
	SD	15.4	12.4	14.3	16.7

Table 3.15 Total U and extractable U contents in the 0–1 and 0–10 cm sediment depths of each cell

		Cell						
	Depth (cm)	1	2	3	4†	5	7†	8†
Total U (mg/kg)	0–1	569.9	436.5	250.5	90.1	225.6	116.0	122.5
	0–10	133.0	133.9	69.4	20.1	47.6	22.2	32.7
Ex. U (mg/kg)	0–1	198.1	295.4	221.3	53.6	175.7	73.3	69.0
	0–10	63.9	84.4	41.3	10.0	32.2	12.0	17.1
Ex. U (% of total)	0–1	34.8	67.7	88.3	59.3	77.9	63.4	52.3
	0–10	48.1	63.1	59.4	50.3	67.6	53.4	51.3

Total U is strongly correlated ($p<0.001$) with total Co, Mn and organic matter (Table 3.10). When data is normalised, stepwise regression (Table 3.13) reveals Mn ($p<0.001$), sediment depth ($p<0.001$) and path length ($p<0.01$) to be the best predictors of U concentration in sediment (Fig 3.5).

On average, between 42–62% of total U is extracted by 0.5 M $NaHCO_3$ (Table 3.14). The pattern to the distribution of extractable U essentially mirrors that of total U with a decrease in concentration being a function of path length, sediment depth and total Mn (Table 3.13).

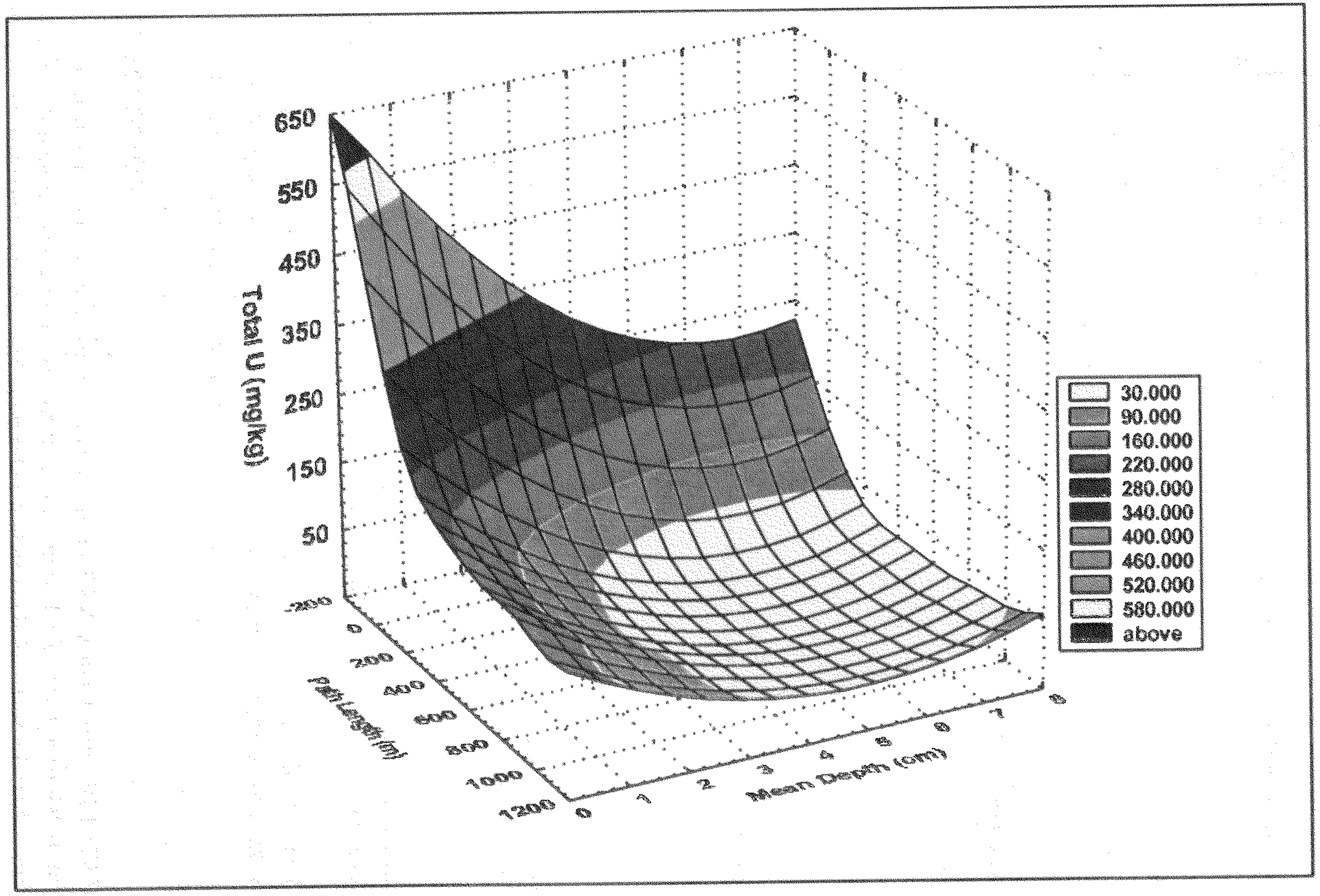

Fig 3.4 Uranium concentration (mg/kg) in sediment of the RP1 CWF as a function of path length (m) and mean depth (cm) of sampling

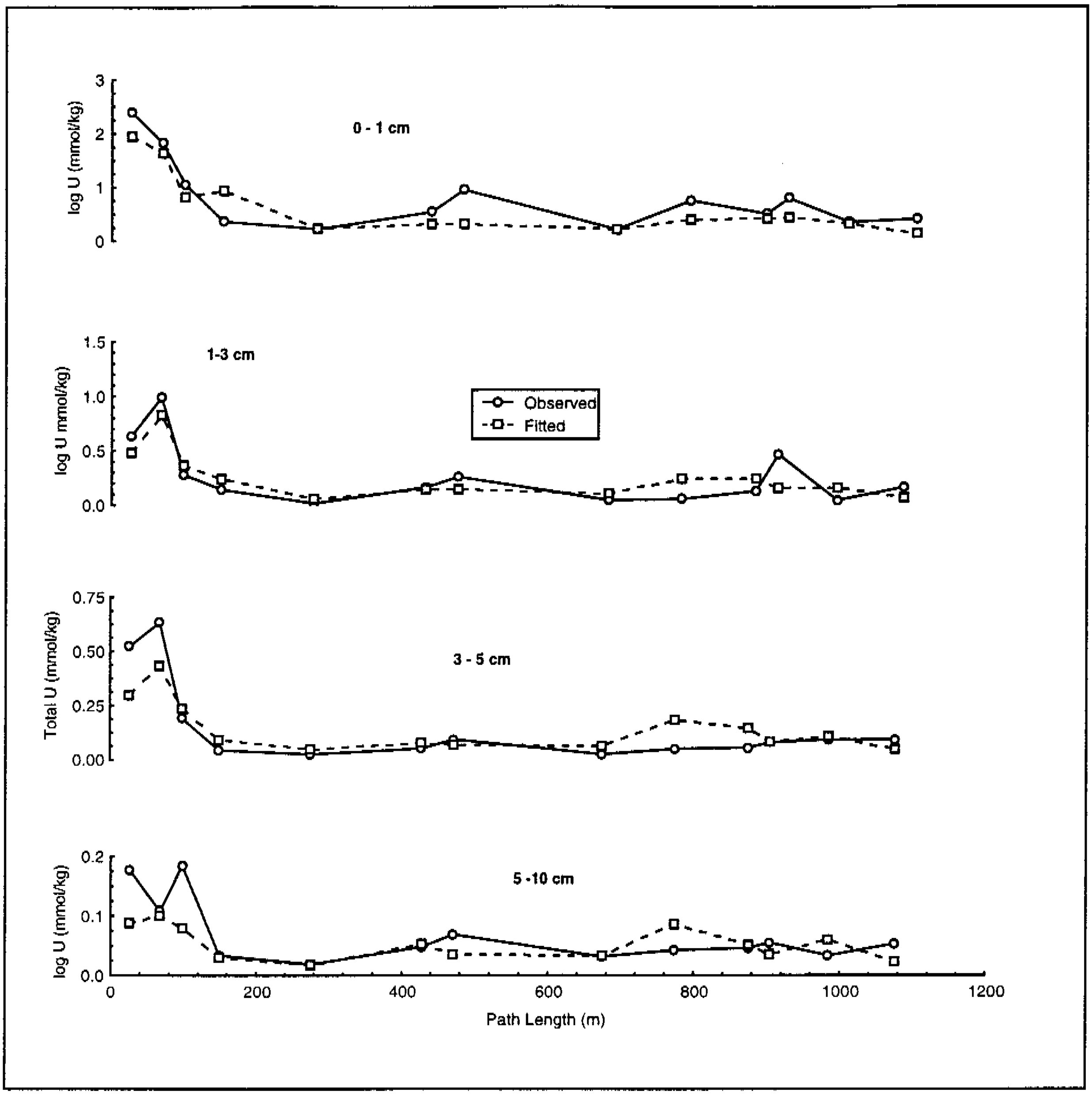

Fig 3.5 Observed and fitted total U concentration in sediment at the 0–1, 1–3, 3–5 and 5–10 cm depths

However, while the highest concentrations of extractable U were found in surface (0–1 cm) sediment of the front three cells (Table 3.13), U extractability by comparison was relatively low in Cell 1 (35%) and at a maximum in Cell 3 (88%).

4 Discussion

The mechanisms by which uranium is removed from RRZ water by the RP1 CWF and its subsequent compartmentalisation are unclear but they have been postulated to involve adsorption to sediment surfaces and suspended matter such as oxy-hydroxides and organic matter, coprecipitation with oxy-hydroxides, and biological uptake (leGras & Klessa 1997). Results presented here suggest that the large majority of retained uranium is accounted for in sediment with around half of the uranium in sediment present in a potentially labile form.

During 1995 and 1996, a total load of 250 kg U (Tables 1.2 & 1.4) was retained by the RP1 CWF. To derive the recovery of retained sediment U in the absence of a control, an estimate was made of the depth of sediment into which U, derived from RRZ water, is dissipated and conserved, and of the background U concentration in sediment. Studies have shown that on the land application at Ranger over 6 years, uranium applied in RRZ water was retained and conserved within the surface 5 cm of soil (Noller & Zhou 1992; Akber & Marten 1992). Sediment in the RP1 CWF is formed on subsoil and a background U concentration was derived from 90–100 cm depth data for control sites on the Magela land application area at Ranger (ERA 1997). Total soil U concentration averages 5 mg/kg and ranges from 1.5-9.5 mg/kg based on ERA (1997) data. Hence, given a background concentration of between 5-10 mg U/kg in sediment and that mine water derived U was retained within the 0-5 cm depth[3], implies a recovery in sediment of approximately 64–77% (159–192 kg U) of the retained U load.

The reactivity of U in RRZ water with the solid phase (ie sediment and particulates) and its retention in the RP1 CWF is dependent on a number of factors with the speciation of U crucially important in determining the nature of the chemical interaction. For example, the affinity of U for adsorption sites on solids is influenced by the charge of U species in solution and that associated with the surface of solids. In each case, pH acts as a master variable dictating the charge properties of both the sorbent and sorbate. To examine how the speciation of soluble U changes in response to pH, the program MINTEQA2 (Brown & Allison 1988) was run. The composition of influent water to the RP1 CWF (Table 4.1) was typified and speciation examined between pH 5–8.5. In addition, the MINTEQA2 database was amended to include U complexes which are not listed in version 3.11. A full list of U species and associated stability constants are given in Table 4.2.

Table 4.1 Composition (M) of the dissolved fraction of RP1CWF influent used in speciation modelling

Constituent	M	Constituent	M
U (as UO_2^{2+})	1.853e-6	Na^+	4.153e-4
Mg^{2+}	4.157e-3	Cl^-	1.072e-4
SO_4^{2-}	4.094e-3	Ca^{2+}	3.994e-4
K^+	7.667e-5	NH_4^+	1.442e-5
NO_3^-	1.856e-4		
Total inorganic C	2.888e-4	Dissolved organic C†	5.000e-6
Mn (as Mn^{2+})	2.786e-6	Fe (as Fe^{2+})	1.702e-7
Cu^{2+}	2.031e-7	Pb^{2+}	2.753e-8
Zn^{2+}	2.969e-7		

†1 mg C/L = 1 x 10^{-6} mole charge

Over the pH range 5.5–8.5, the chemistry of U(VI) in process water of the RP1CWF is characterised by carbonato complexes of 0, -1, -2 and -4 valences (Fig 4.1) two of which, $UO_2CO_3^0$ and $UO_2(CO_3)_2^{2-}$, dominate. The complexation of U (as the uranyl ion) by dissolved organic matter appears to be only important at <pH 6, as does the formation of the ion pair, $UO_2SO_4^0$, and the first product of the hydrolysis of the uranyl ion, UO_2OH^+. Chloro-, nitrate, hydroxy- (other than UO_2OH^+) and polymeric complexes of U(VI) have very low activities over the pH 5–8.5 range and are not important.

---

[3] Assuming 2500 t OD sediment per hectare in the 0–15 cm depth.

The sequestration of U(VI) from solution by soil and sediment is incompletely understood. However, the mobility of U (VI) is known to be maximised under oxidising, carbonate-rich and high ionic strength conditions (Amonette et al 1994) which favour the zero and negatively charged carbonato complexes in solution and/or the replacement of the uranyl ion from exchange sites by alkaline earth metals (Amonette et al 1994). Maximum adsorption of uranium on the Fe oxy-hydroxides hematite, ferrihydrite and goethite occurs around pH 6–7 (Ho & Miller 1986; Waite et al 1992; Duff & Amrhein 1996) with the pH edge sensitive to the partial pressure of CO_2 (ρ_{CO_2}). An increase in ρ_{CO_2} results in a lowering of the pH edge (Waite et al 1992) and domination of aqueous U chemistry by the di- and tri-carbonato complexes (Waite et al 1992; Duff & Amrhein 1996). Results from surface complexation modelling of hematite and goethite suggest that it is the hemi-carbonate form ($[UO_2]_2[OH]_3CO_3^-$) which is actively adsorbed by these oxyhydroxides in carbonate systems with proportionally less U being adsorbed at higher pH because of the formation of the $UO_2(CO_3)_2^{2-}$ and $UO_2(CO_3)_3^{4-}$ species (Ho & Miller 1986; Duff & Amrhein 1996). In

Table 4.2 List of U (VI) complexes and log K stability constants used in determining U (VI) speciation

Complex	Log K	Notes on log K††
$UO_2^{2+} + Cl^- = UO_2Cl^+$	0.22	1
UO_2^{2+} + DOM = UO_2-DOM	6.5†	2
$UO_2^{2+} + SO_4^{2-} = UO_2SO_4^0$	2.709	1
$UO_2^{2+} + 2SO_4^{2-} = UO_2(SO_4)_2^{2-}$	4.183	1
$UO_2^{2+} + NO_3^- = UO_2NO_3^+$	-0.08	4
$UO_2^{2+} + 2NO_3^- = UO_2(NO_3)^0$	-0.71	4
$UO_2^{2+} + 3NO_3^- = UO_2(NO_3)_3^-$	0.32	4
$UO_2^{2+} + H_2O = UO_2OH^+ + H^+$	-5.09	1
$3UO_2^{2+} + 5H_2O =(UO_2)_3(OH)_5^+ +5H^+$	-15.593	1
$4UO_2^{2+} + 7H_2O = (UO_2)_4(OH)_7^+ + 7H^+$	-21.9	3
$3UO_2^{2+} + 3H_2O + CO_3^{2-} = (UO_2)_2CO_3(OH)_3^+ + 3H^+$	1.01	4
$2UO_2^{2+} + 2H_2O = (UO_2)_2(OH)_2^{2+} +2H^+$	-5.645	1
$3UO_2^{2+} + 4H_2O =(UO_2)_3(OH)_4^{2+} +4H^+$	-11.9	3
$2UO_2^{2+} + H_2O = (UO_2)_2OH^{3+} + H^+$	-2.8	3
$UO_2^{2+} + H_2O = UO_2(OH)_2^0 +2H^+$	-12.0	3
$UO_2^{2+} + 3H_2O = UO_2(OH)_3^- + 3H^+$	-20.0	3
$3UO_2^{2+} + 7H_2O =(UO_2)_3(OH)_7^- +7H^+$	-31.0	3
$UO_2^{2+} + 4H_2O = UO_2(OH)_4^{2-} + 4H^+$	-33.0	3
$UO_2^{2+} + CO_3^{2-} = UO_2CO_3^0$	10.071	1
$UO_2^{2+} + 2CO_3^{2-} = UO_2(CO_3)_2^{2-}$	17.008	1
$UO_2^{2+} + 3CO_3^{2-} = UO_2(CO_3)_3^{4-}$	21.384	1
$3UO_2^{2+} + 6CO_3^{2-} = (UO_2)_3(CO_3)_6^{6-}$	53.71	4
$2UO_2^{2+} + 3H_2O + CO_3^{2-} = (UO_2)_2CO_3(OH)_3^- + 3H^+$	-1.2	3
$11UO_2^{2+} + 12H_2O + CO_3^{2-} = (UO_2)_{11}(OH)_{12}(CO_3)_6^{2-} + 12H^+$	36.44	4

†Standard deviation = 0.8; ††note(1): Minteqa2 database, note(2): Giesy et al (1986), note(3): Grenthe et al (1992); cited by Duff & Amrhein (1996), note(4): derived from Bennett & Read (1992).

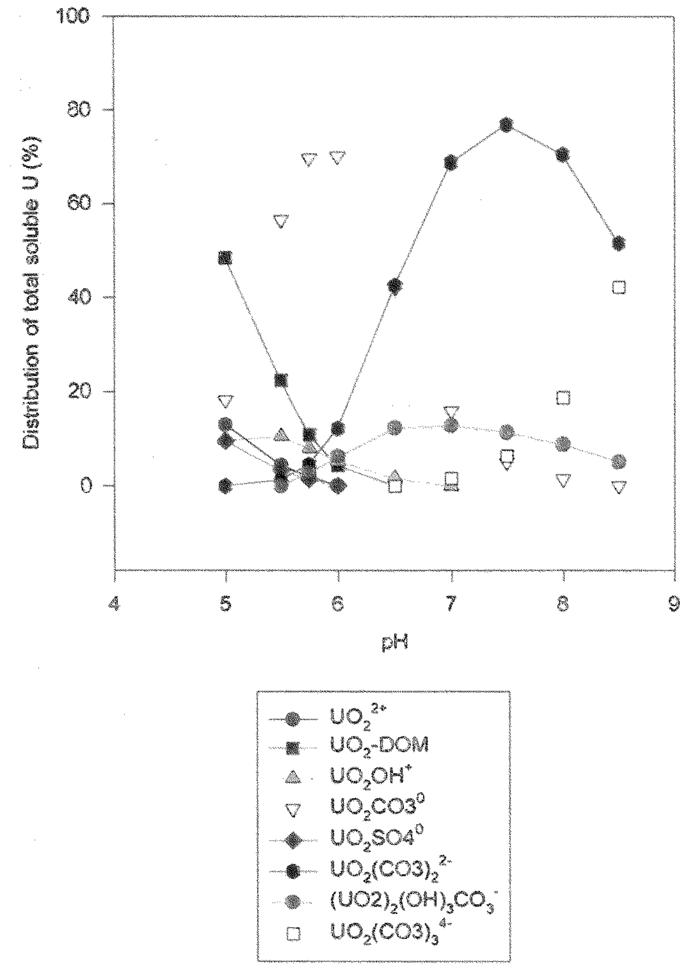

Fig 4.1 Effect of pH on the speciation of U in the influent water of the RP1CWF

carbonate-free systems, adsorption of monomeric U as UO_2^{2+} best describes interaction with Fe oxy-hydroxides (Hsi & Langmuir 1985) and smectite (Chisholm-Brause et al 1994).

The pH of RP1CWF cell water during the Dry season process period typically varies between 6.8-8.0 (ERA 1997) although in 1995, after Pit # 1 storage of RRZ water, pH values as high as 9 were recorded for a short time (ERA 1996). Hence, the virtual absence of cationic forms of U(VI) in solution above pH 7 does not favour, superficially at least, the retention of U as outer-sphere complexes on the surfaces of organic matter and clay, and on oxyhydroxides at a pH above their point of zero charge. Although speciation modelling predicts that carbonato complexes are the principle forms of U in solution at the ambient pH of the water column, the acidic pH of sediment (Tables 3.1 & 3.2) will lead to lower pH values in pore water compared to the water column and favour the formation of the mononuclear species, UO_2^{2+} and UO_2OH^+.

It is likely that adsorption and coprecipitation of U by colloids as well as sorption by sediment surfaces determine the removal of U from solution in the RP1 CWF (leGras & Klessa 1997). We have postulated, based on an examination of rate loss equations of particulate and soluble U, Fe and Mn in the RP1 CWF, that U removal is probably more influenced by Fe rich particulates than by colloidal Mn. In the weathered regolith, it is well known that Fe oxyhydroxides act as scavengers of U (Koons et al 1980; Edis 1991). For example at Koongarra, the majority of U in both the primary and secondary ore bodies is associated with crystalline hematite and goethite (Murakami et al 1992). In weathered rock, U can also be found associated with Mn oxides (Koppi et al 1996) especially on the surface of fissures and remnant schistosity (Edis 1991; Koppi & Klessa 1991) which typify well-oxidised zones. The work we report here shows that there is a significant (P<0.001) correlation between Mn and U in the sediments of the RP1 CWF (Fig 4.2) with around 71% of the variation in total U explained by total Mn, path length and sediment depth (Table 3.13). The fitted multiple regression relationship is shown graphically for 1, 2 and 5 mmol Mn/kg at the 1, 5 and 10 cm sediment depths in Figure 4.3.

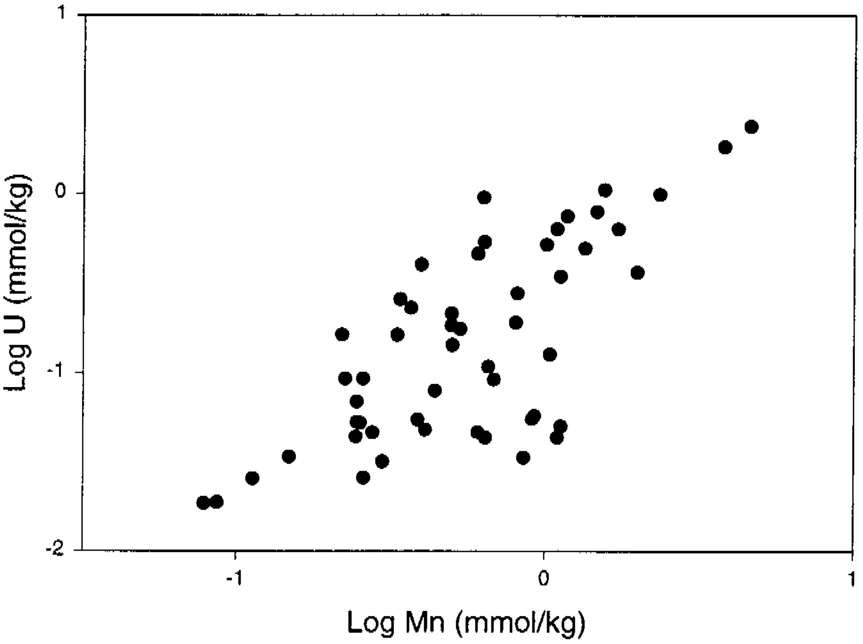

Fig 4.2 Scatterplot of Total U versus Total Mn

However, it is important to note that the correlation of Mn with U in sediment need not imply that Mn oxides are sequestering U. A similar trend would be seen if autocorrelation was being demonstrated with the removal of both U and Mn driven by similar kinetics during the polishing process. Further work is needed to elucidate whether U in RP1 CWF sediment is associated with Mn oxides.

There is no agreed or accepted procedure to measure bioavailable U in soil or sediment. Relatively little work has been reported dealing with the suitability of sediment/soil extractants and/or chemical procedures to measure the (bio)availability or lability of uranium. Amonette et al (1994) reviewed the literature and provided recommendations on the extraction of *total environmentally available uranium* (TAU) and subclasses *readily available uranium* (RAU), *slowly available uranium* (SAU) and *very slowly available*

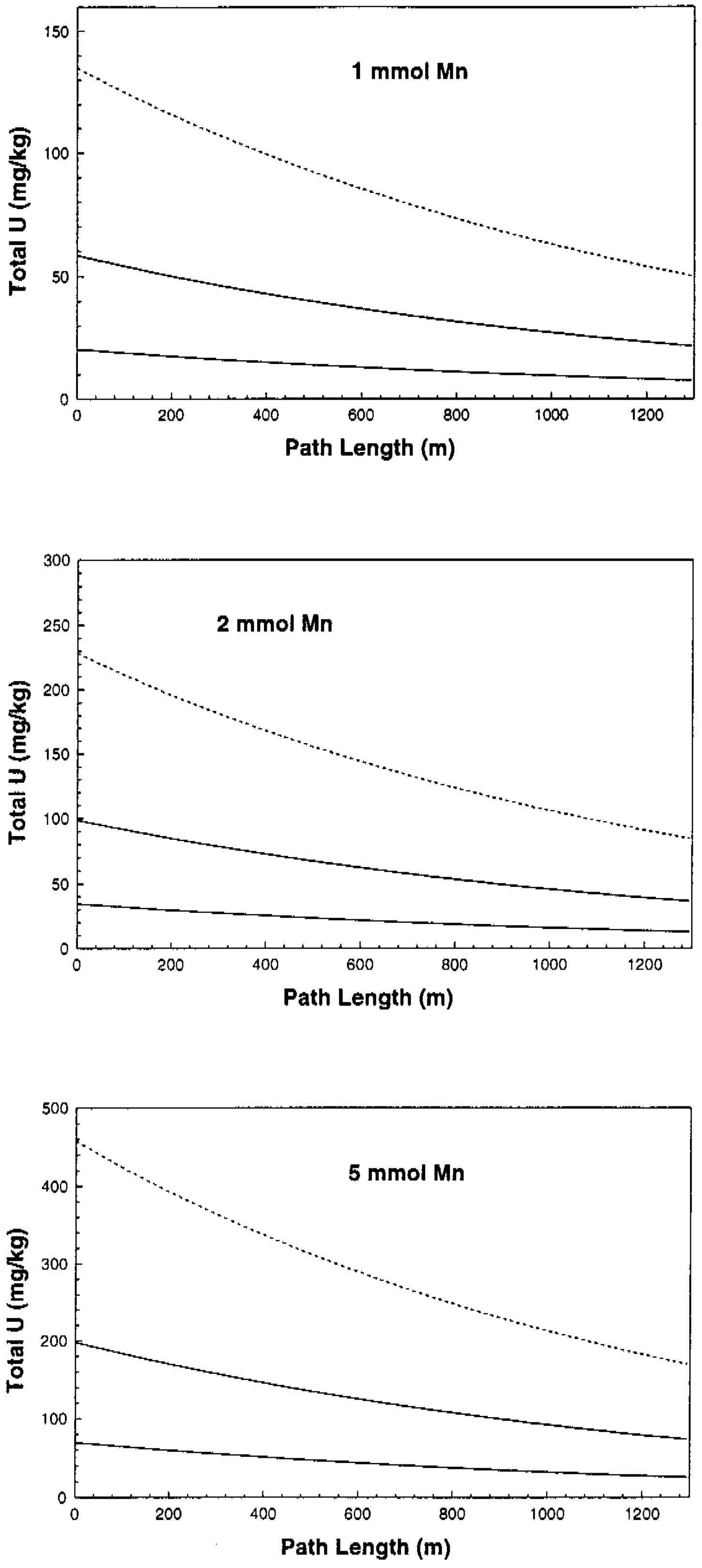

Fig 4.3 Total U concentration in sediment as a best fit function of total Mn concentration (1, 2 and 5 mM/kg), path length (m) and depth (top-1 cm; middle-5 cm; bottom-10 cm)

uranium (VSAU) in soil and sediment. TAU is determined using 5% HCl as an extractant, followed by analysis of U, then digestion of the residue with 30% H_2O_2 to convert U(IV) to U(VI) and further U determination. RAU is operationally defined using 0.1 M CH_3COOH extraction, and SAU by an oxidising extraction in a carbonate buffer (0.1 M $NaHCO_3$ + H_2O_2). VSAU is determined by difference where;

$$VSAU = TAU - (RAU + SAU)$$

and where RAU and SAU are determined sequentially on the same sample.

Of the procedures recommended by Amonette et al (1994), the derivation of the SAU fraction bears closest to the extractant and method we have used although in our case a single extraction would have removed both weakly and more strongly held U (ie equivalent to RAU + SAU). Importantly, however, Amonette et al (1994) indicate that their recommended procedure for SAU in soil and sediment remains to be tested and evaluated against biological uptake criteria. They also concluded from a review of the literature that the little work which has been done on the *environmental availability* of uranium had not attempted to predict the availability of U and that there was a shortfall of information relating the extractability of U to bioavailability.

Ostensibly, $NaHCO_3$ buffered at pH 8.5 (ie as used for Olsen extractable P) is an attractive soil extractant to remove bioavailable U. Soil and sediment pore waters are often characterised by relatively high dissolved CO_2 concentration which will have an important influence on the carbonato speciation of U and hence its environmental fate. The combination of alkaline pH and high bicarbonate concentration encourages desorption of U into the aqueous phase with the formation of the stable mono- and di-uranium carbonato complexes (refer to earlier discussion) which will remain in solution. An extraction at a fixed pH reduces variation in the extractability of U arising from soil pH effects and under alkaline conditions will encourage an extended conformation of humic acid and its desorption from soil particle surfaces including oxyhydroxides (Ho & Miller 1985). Consequently, U adsorption sites on organic matter, clays and oxyhydroxides are opened up to contact with the aqueous phase and extraction. Hence, it is probable that bicarbonate extraction will remove U involved in both outer sphere binding (ie exchangeable U) and inner sphere coordination (ie residual U) representing a range of bonding energies with soil surfaces. In our review of the literature, we found only one study where 0.5 M $NaHCO_3$ (pH 8.5) was used in an environmental study to measure soil U. Sheppard & Evenden (1985) extracted soil with 0.5 M $NaHCO_3$ (pH 8.5) to remove Tc, P and U from spiked lysimeters and found a mean extractability of 42%. This compares with an average for all sediment samples in the RP1 CWF of 51% (±17%) and a range of 21–88%. Further work is recommended to clarify the forms of sediment and soil U which are extracted by bicarbonate and their relative bioavailabilities.

Cobalt is strongly correlated with Mn (Fig 4.4) with the highest Co concentration in surface sediment found in the front three cells (Table 3.10). However, most sediment Co in the RP1 CWF is native and not derived from RP2 effluent. This is implied because the concentration of Co in RP2 water is unlikely to exceed 2 µg/L[4]. Hence the Co load to the RP1 CWF over 1995 and 1996 would have amounted to less than 1.3 kg and this load is more than accounted for in the surface 0–1 cm sediment of the whole of the wetland filter.

---

[4] In the absence of published or reported data for Co in RP2 waters, this concentration is based on semi-quantitative ICPMS scans of RP2 water conducted by ***eriss*** in 1989.

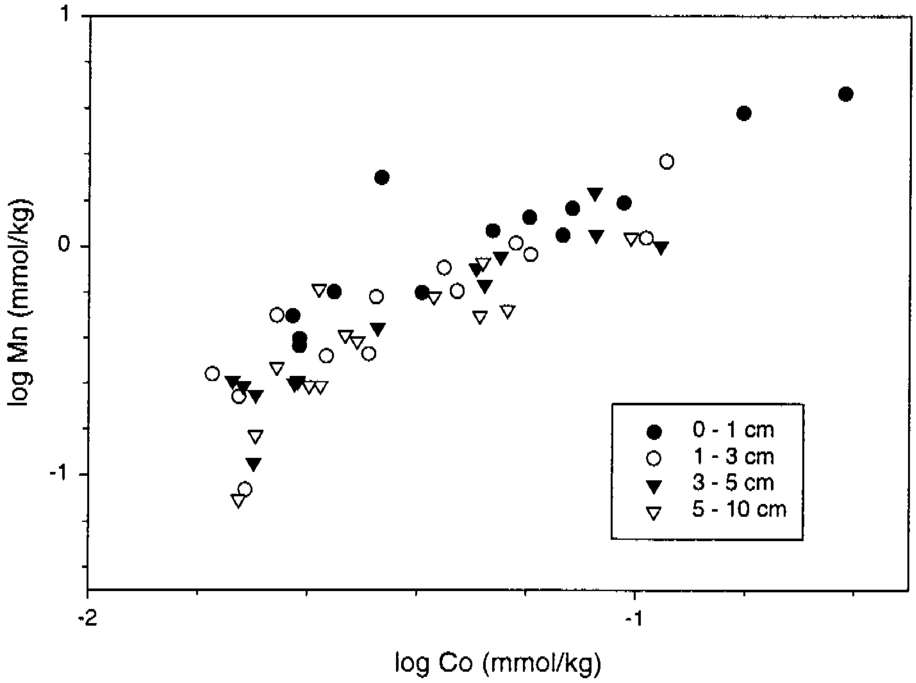

Fig 4.4 Scatterplot of total Mn versus total Co in sediment

The association of Co with Mn in the sediments of the wetland filter is to be expected. Manganese oxides strongly adsorb Co (Murray 1975a,b; Murray & Dillard 1979) and, in soil, most Co is associated with oxyhydroxides, particularly Mn oxides (McLaren et al 1986). The similar pattern to Co and Mn distribution in the surface sediment of Cells 1, 2 and 3 supports the hypothesis that Mn colloids floc out quickly once RP2 water enters the wetland filter. According to leGras & Klessa (1997), around half the Mn load in RP2 effluent is removed within approximately the first 300 m of the RP1 CWF, assuming a retention time of 11 days and steady state conditions. There is also some evidence from stoichiometry that may infer that the mode of origin of the mineral phases containing Co and Mn in the surface 0–1 cm sediment differs from deeper samples (Table 4.3).

Table 4.3 Mean Co/Mn ratios (mmol/kg) in sediment samples taken at various depths (n = 13)

Depth (cm)	0–1	1–3	3–5	5–10
Mean	0.051	<u>0.081</u>	<u>0.086</u>	<u>0.099</u>
SE		0.010		

Underlined means are not significantly different (P>0.05).

Conclusion

The study described here forms a part of a larger continuing project concerned with the processes involved and factors affecting the efficacy of constructed wetland filters to polish mine waters at Ranger. While attention to date has largely focussed on the performance of the RP1 CWF in removing contaminants (ERA 1996a, 1997), and the associated chemical kinetics of these processes in solution (leGras & Klessa 1997), there has been little information upon which to develop an understanding of the fate of the contaminants so removed. This is important because the compartmentalisation and turnover of contaminants within the filter has ramifications both for the capacity of wetland systems to retain contaminants and for their efficient operation over the long term.

Sediment in the RP1 CWF was found to be moderate to slightly acidic (pH 4.6–6.5), and to have a very low to moderate CEC (0.4–11.3 cmol_+/kg) and low organic C content (0.6–1.6%). The low organic matter content reflects the immaturity of the system which in turn has implications for adsorptive capacity, turnover of contaminants and the performance of the filter over time.

Total U concentration decreased in an approximately exponential fashion with path length and depth from a maximum of 570 mg/kg in Cell 1 surface sediment. On average, 51% of total U was extracted by bicarbonate. It was estimated that roughly 64–77% of the retained U load from the polishing of RP2 water could be accounted for in the sediment of the wetland filter. Further work is required to verify the recovery of the retained U load in sediment and to ascertain the fate of the remainder. In addition, further study is needed to determine the lability of sediment U.

The more acidic pH of sediment pore water and its higher partial pressure of CO_2 compared to the overlying water column, will favour the speciation and sorption of the mononuclear cation and hemicarbonate forms of U which are adsorbed preferentially by oxyhydroxide surfaces. Total U was highly correlated with total Mn which might imply the active sequestering of U by Mn oxide surfaces. A similarly high correlation was found between total Mn and Co which was attributed largely to native soil minerals. However, the relative enrichment of surface sediment by Mn and Co, especially in the front cells, suggests that the formation of Mn oxides and the sorption of Co is an active process.

References

Akber RA and Marten R 1992. Fate of radionuclides applied to soil in the Ranger uranium mine land application area. In: *Proceedings of the Workshop on Land Application of Effluent Water from Uranium Mines in the Alligator Rivers Region, Jabiru, 11–13 September 1991*, 139–165, Australian Government Publishing Service, Canberra.

Amonette JE, Holdren GR, Krupa KM & Lindenmeier CW 1994. *Assessing the environmental availability of uranium in soils and sediments*. NUREG/CR-6232, PNL-9750. Pacific Northwest Laboratory, US Nuclear Regulatory Commission, Washington, DC.

Bennett DG & Read D 1992. *Geochemical Data Bases.* Alligator Rivers Analogue Project Final Report Vol 10, Australian Nuclear Science and Technology Organisation, Sydney.

Brown DS & Allison JD 1988. *MINTEQA1, an equilibrium metal speciation model: User's manual.* Report No. EPA/600/3-87/012, United States Environmental Protection Agency, Athens, Georgia.

Chisholm-Brause C, Conradson SD, Buscher CT, Eller PG and Morris DE 1994. Speciation of uranyl sorbed at multiple binding sites on montmorillonite. *Geochimica Cosmochimica Acta* **58**, 3625–3621.

Duff MC & Amrhein C 1996. Uranium (VI) adsorption on goethite and soil in carbonate solutions. *Soil Science Society of America Journal* **60**, 1393–1400.

Edis R 1991. *The effect of weathering on the distribution of uranium and associated elements at Koongarra, Northern Territory, Australia.* M. Sc. Agr. Thesis, Department of Soil Science, University of Sydney.

Energy Resources of Australia 1996a. *Environmental annual report 1996.* Energy Resources of Australia Ltd.

Energy Resources of Australia 1996b. *Wetland filter performance report 1995.* Energy Resources of Australia Ltd.

Energy Resources of Australia 1997. *Environmental annual report 1997.* Energy Resources of Australia Ltd.

Fuller JPH 1997. Acid persulphate digest for soil total phosphorus. *Internet http://ash.ecology.uga.edu/soil-tp.html* (as at 17/3/97).

Giesy JP, Geiger RA & Kevern NR 1986. UO_2^{2+}–Humate interactions in soft, acid, humate-rich waters. *Journal of Environmental Radioactivity* **4**, 30–64.

Grenthe I, Fuger J, Konings R, Lemire RJ, Muller AB, Nguyen-Trung C & Wanner J 1992. *The Chemical Thermodynamics of Uranium.* Elsevier, New York.

Hesse PR 1971. *A textbook of soil chemical analysis.* John Murray, London.

His CD & Langmuir D 1985. Adsorption of uranyl onto ferric oxyhydroxides: Application of the surface complexation site-binding model. *Geochimica Cosmochimica Acta* **49**, 1931–1941.

Ho CH & Miller NH 1985. Adsorption of uranyl species from bicarbonate solution onto hematite particles. *Journal of Colloid and Interface Science* **110**, 165–171.

Ho CH & Miller NH 1985. Effect of humic acid on uranium uptake by hematite particles. *Journal of Colloid and Interface Science* **106**, 281–288.

Koons RD, Helmke PA and Jackson ML 1980. Association of trace elements with iron oxides during weathering. *Proceedings of the Soil Science Society of America* **44**, 155–159.

Koppi AJ, Edis R, Field DJ, Geering HR, Klessa DA and Cockayne DJH 1996. Rare earth element trends and cerium-uranium-manganese associations in weathered rock from Koongarra, Northern Territory, Australia. *Geochimica Cosmochimica Acta* **60**, 1695–1707.

Koppi AJ & Klessa DA 1991. Uranium and cerium associations in the M2 profile at Koongarra. *In* P Duerden (ed) Alligator Rivers Region Project Progress Report (1 March 1991–31 August 1991), Australian Nuclear Science and Technology Organisation, pp 239–246.

leGras CAA & Klessa DA 1997. *An assessment of the performance of the Ranger RP1 constructed wetland filter during releases in 1995 and 1996.* Internal Report **255**, Supervising Scientist.

McLaren RG, Lawson DM & Swift RS 1986. Sorption and desorption of cobalt by soils and soil components. *Journal of Soil Science* **37**, 413–426.

Murakami T, Isobe H, Ohnuki T, Yanase N, Sato T, Kimura H, Sekine K, Edis R, Koppi AJ, Klessa DA, Conoley C, Nagano T, Nakashima S & Ewing RC 1992. *Weathering and its effect on uranium redistribution.* Alligator Rivers Analogue Project Volume **9**, DOE/HMIP/RR/92/079, Australian Nuclear Science and Technology Organisation.

Murray JW 1975a. The interaction of metal ions at the manganese dioxide-solution interface. *Geochimica et Cosmochimica* **39**, 505–519.

Murray JW 1975b. The interaction of cobalt with hydrous manganese dioxide. *Geochimica et Cosmochimica* **39**, 635–647.

Murray JW & Dillard JG 1979. The oxidation of cobalt (II) adsorbed on manganese dioxide. *Geochimica et Cosmochimica* **43**, 781–787.

Nisbet H. 1995. Wetland filtration research at ERA Ranger Mine. In: *Wetland research in the wet-dry tropics of Australia.* Finlayson C. M. (ed) 165-172, Supervising Scientist Report **101**, Commonwealth of Australia.

Noller BN and Zhou JX 1992. Land application at Ranger Uranium Mine, Northern Australia: Six years review. In: *Proceedings of the Workshop on Land Application of Effluent Water from Uranium Mines in the Alligator Rivers Region, Jabiru, 11–13 September 1991*, 107–112, Australian Government Publishing Service, Canberra.

Rayment GE & Higginson FR 1992. *Australian Laboratory Handbook of Soil and Water Chemical Methods.* Inkata Press, Melbourne.

Sheppard SC & Evenden WG 1985. Mobility and uptake by plants of elements placed near a shallow water table interface. *Journal of Environmental Quality* **14**, 554–560.

Waite TD, Payne TE, Davis JA & Sekine K 1992. *Uranium sorption.* Alligator Rivers Analogue Project Volume **13**, DOE/HMIP/RR/92/0823, Australian Nuclear Science and Technology Organisation.

Appendix

Table A1 Sediment pH, EC, exchangeable bases, cation exchange capacity (CEC), total nitrogen, total carbon, total phosphorus and available phosphorus.

Table A2 Total Cd, Co, Cu, Fe, Mn, Pb U and Zn, and extractable U in sediment.

Table A1 Sediment pH, EC, exchangeable bases cation exchange capacity (CEC), total nitrogen, total carbon, total phosphorus and available phosphorus.

Cell	Depth (cm)	pH	EC (µS/cm)	Mg (cmol$_+$/kg)	Ca (cmol$_+$/kg)	K (cmol$_+$/kg)	Na (cmol$_+$/kg)	CEC (cmol$_+$/kg)	Total N (%)	Total C (%)	Total P (%)	Available P (mg/kg)
1	0–1	5.29	126	3.04	0.71	0.09	0.08	5.74	0.121	1.609	0.028	1.56
	1–3	5.78	74	2.09	0.46	0.16	0.06	6.62	0.032	0.619	0.022	1.04
	3–5	5.85	65	2.01	0.52	0.05	0.03	3.89	0.025	0.604	0.021	0.78
	5–10	6.20	33	1.58	0.32	0.03	0.02	5.41	0.015	0.363	0.018	0.78
2	0–1	6.27	158	2.75	0.66	0.09	0.03	5.93	0.070	1.089	0.034	2.46
	1–3	6.18	124	2.65	0.53	0.06	0.03	4.03	0.034	0.689	0.022	1.81
	3–5	6.35	85	2.14	0.44	0.06	0.04	0.90	0.019	0.509	0.023	1.29
	5–10	6.40	66	1.86	0.34	0.07	0.03	1.49	0.011	0.377	0.016	0.91
3	0–1	4.81	266	2.31	0.46	0.07	0.02	5.80	0.047	0.887	0.020	1.81
	1–3	4.64	152	1.22	0.24	0.04	0.02	6.07	0.008	0.422	0.019	1.23
	3–5	6.05	51	1.97	0.47	0.05	0.02	2.66	0.003	0.468	0.020	1.04
	5–10	6.35	69	2.33	0.37	0.04	0.04	3.92	0.002	0.377	0.016	1.04
4 (inlet)	0–1	5.97	60	1.47	0.34	0.05	0.01	2.63	0.030	0.622	0.013	1.23
	1–3	6.11	33	1.24	0.33	0.05	0.04	3.75	0.014	0.583	0.011	1.03
	3–5	6.30	27	1.18	0.22	0.04	0.06	3.49	0.020	0.627	0.009	1.36
	5–10	6.30	22	1.07	0.13	0.30	0.03	3.68	0.020	0.424	0.008	1.29
4 (middle)	0–1	5.81	74	1.35	0.30	0.05	0.03	3.06	0.033	0.737	0.008	1.29
	1–3	5.67	34	0.81	0.13	0.03	0.01	1.12	0.035	0.480	0.006	1.29

	3–5	5.40	54	0.83	0.11	0.03	0.02	1.77	0.036	0.599	0.006	1.16
	5–10	5.24±0.03	57±2	0.78	0.08	0.03	0.01	0.95	0.026	0.553	0.006	1.16
4 (outlet	0–1	6.47	103	2.37	0.31	0.20	0.10	1.57	0.045	0.804	0.016	2.22
	1–3	5.97	45	2.08	0.15	0.08	0.02	5.46	0.017	0.526	0.018	1.69
	3–5	5.88	55	2.49	0.19	0.03	0.07	2.54	0.014	0.477	0.017	1.56
	5–10	5.51	100	2.73	0.44	0.08	0.03	3.97	0.009	0.267	0.013	1.63
5	0–1	5.03	176	2.24	0.26	0.08	0.05	1.81	0.099	1.450	0.014	2.62
	1–3	5.40	61	1.23	0.29	0.04	0.06	4.66	0.037	0.635	0.012	2.09
	3–5	5.55	44	1.34	0.27	0.16	0.05	2.27	0.024	0.536	0.010	1.56
	5–10	5.56±0.02	55±1	1.24	0.27	0.03	0.06	1.64	0.022	0.668	0.009	1.37
7 (inlet)	0–1	5.19	116	2.25	0.48	0.09	0.05	4.62	0.029	0.569	0.012	1.61
	1–3	5.95	34	1.75	0.18	0.06	0.02	3.05	0.008	0.635	0.012	1.13
	3–5	5.72±0.01	38±6	1.20	0.15	0.06	0.04	8.71	0.006	0.800	0.009	1.40
	5–10	5.96	31	2.08	0.52	0.10	0.01	3.90	0.005	0.652	0.012	1.40
7 (middle)	0–1	5.44	101	2.06	0.32	0.08	0.03	4.79	0.048	1.473	0.014	1.81
	1–3	6.01	52	2.57	0.28	0.07	0.02	1.23	0.016	0.914	0.013	1.26
	3–5	5.50	89	5.22	0.13	0.12	0.06	5.53	0.003	0.566	0.012	1.27
	5–10	5.28±0.04	91±4	6.49	0.62	0.16	0.10	6.75	0.004	0.559	0.011	1.00
7 (outlet)	0–1	5.39	135	2.36	0.46	0.16	0.04	4.19	0.057	1.116	0.014	1.13
	1–3	6.15	46	2.10	0.30	0.10	0.03	1.77	0.013	0.896	0.012	1.40
	3–5	5.73	80	1.93	0.29	0.09	0.01	2.72	0.011	0.856	0.012	1.26
	5–10	5.36	86	2.69	0.72	0.10	0.04	5.57	0.003	0.745	0.012	1.26
8 (inlet)	0–1	5.14	188	4.94	1.10	0.12	0.09	11.13	0.060	1.611	0.023	1.14

	1–3	5.72	81	2.41	0.45	0.06	0.03	5.11	0.022	0.719	0.012	2.22
	3–5	5.94	77	3.60	0.37	0.07	0.04	5.71	0.019	0.599	0.014	1.40
	5–10	5.80	81	3.02	0.28	0.05	0.03	4.05	0.012	0.690	0.014	1.27
8 (middle)	0–1	6.17	92	2.96	0.50	0.21	0.07	6.81	0.062	1.212	0.013	1.26
	1–3	5.85	45	1.69	0.34	0.03	0.01	3.29	0.025	0.949	0.010	1.46
	3–5	5.85	60	1.51	0.34	0.04	0.00	4.66	0.033	0.829	0.009	1.24
	5–10	5.64	101	1.32	0.28	0.02	0.01	5.64	0.026	0.965	0.010	1.11
8 (outlet)	0–1	5.11	72	1.61	0.33	0.07	0.00	5.05	0.026	0.854	0.013	1.11
	1–3	5.50	44	1.75	0.26	0.06	0.01	3.50	0.016	0.552	0.012	1.37
	3–5	5.78	42	1.60	0.24	0.06	0.01	5.24	0.024	0.680	0.013	1.37
	5–10	5.56±0.04	48±2	1.53	0.23	0.05	0.01	6.19	0.007	0.584	0.012	1.51

Table A2 Total Cd, Co, Cu, Fe, Mn, Pb U and Zn, and extractable U in sediment

Cell	Depth (cm)	Total Cd (mg/kg)	Total Co (mg/kg)	Total Cu (mg/kg)	Total Fe (%)	Total Mn (mg/kg)	Total Pb (mg/kg)	Total U (mg/kg)	Extractable U (mg/kg)	Total Zn (mg/kg)
1	0–1	0.06	14.17	37.18	3.03	251.48	13.94	569.87	198.1	47.56
	1–3	0.03	6.13	13.75	1.61	59.91	6.95	150.63	96.9	19.16
	3–5	0.02	6.52	18.99	1.51	55.26	5.36	124.18	61.4	23.84
	5–10	0.00	3.42	14.96	1.31	29.07	6.04	42.04	24.9	11.03
2	0–1	0.04	9.22	39.09	2.11	207.38	8.38	436.53	295.4	31.18
	1–3	0.02	6.67	34.55	2.01	128.48	8.43	235.99	157.6	21.99
	3–5	0.02	4.93	23.01	1.91	94.49	8.43	150.63	79.0	14.64
	5–10	0.01	1.55	7.13	1.91	35.81	8.65	25.81	15.2	5.10
3	0–1	0.03	5.58	17.28	1.61	85.26	6.52	250.48	221.3	19.86
	1–3	0.19	2.62	12.08	1.71	44.31	7.45	66.46	33.3	27.19
	3–5	0.03	3.00	10.74	2.41	43.95	10.42	45.67	16.2	48.69
	5–10	0.02	3.05	12.35	2.34	27.27	9.98	43.96	18.5	23.74
4 (inlet)	0–1	0.03	2.01	11.65	1.52	109.05	9.95	87.13	46.6	20.32
	1–3	0.02	1.30	6.84	1.16	27.52	7.69	34.13	21.1	7.80
	3–5	0.00	1.13	9.05	1.17	13.36	7.57	10.42	4.2	10.88
	5–10	0.01	1.19	17.43	1.15	8.17	7.61	8.04	2.6	9.58
4 (middle)	0–1	0.01	1.43	11.40	1.14	20.10	8.12	55.32	34.2	8.23

	1–3	0.01	1.14	3.57	0.80	4.76	6.71	4.47	3.0	4.11
	3–5	0.00	1.18	5.45	0.86	6.21	6.92	6.09	1.6	4.87
	5–10	0.00	1.11	5.23	0.88	4.32	6.84	4.42	1.4	13.07
4 (outlet	0–1	0.03	1.65	11.43	2.87	34.77	12.27	127.90	80.1	8.21
	1–3	0.02	1.60	8.33	3.21	18.16	13.66	38.95	19.3	3.49
	3–5	0.02	1.40	13.45	3.11	13.78	12.65	12.49	4.2	4.80
	5–10	0.02	1.73	25.04	3.83	22.44	15.90	11.42	2.7	7.90
5	0–1	6.56	2.39	18.90	1.32	34.46	47.92	225.63	175.7	734.96
	1–3	1.87	1.91	11.03	1.28	18.55	19.37	61.70	33.7	207.38
	3–5	0.11	1.19	5.82	0.82	12.30	6.65	22.15	16.2	15.08
	5–10	0.08	1.56	9.74	0.98	13.46	7.91	16.43	9.3	11.42
7 (inlet)	0–1	0.41	1.39	10.41	1.79	27.28	11.69	51.42	32.7	50.05
	1–3	0.53	0.99	8.37	1.74	15.13	9.68	11.09	6.2	12.10
	3–5	0.09	1.08	7.08	1.53	14.15	8.40	6.14	2.1	3.60
	5–10	0.04	1.30	7.99	2.22	16.27	11.11	7.55	2.4	4.60
7 (middle)	0–1	0.07	3.21	14.49	2.31	64.41	11.67	178.20	110.7	14.86
	1–3	0.02	3.77	38.23	3.09	50.66	11.82	13.66	8.0	18.35
	3–5	0.03	4.97	25.36	4.33	61.72	17.20	11.93	3.3	12.05
	5–10	0.06	5.75	27.50	4.18	60.16	15.58	10.32	2.4	9.60
7 (outlet)	0–1	0.11	3.75	22.60	2.96	73.80	12.40	118.50	76.6	23.73

	1–3	0.05	3.54	29.29	2.57	56.81	11.56	30.21	21.3	17.97
	3–5	0.03	3.32	19.74	2.95	49.80	12.91	13.13	6.7	9.56
	5–10	0.02	2.51	23.10	3.39	33.15	14.06	11.05	4.2	7.43
8 (inlet)	0–1	1.13	4.49	31.66	4.26	80.56	24.45	188.11	131.1	150.57
	1–3	0.76	1.97	22.31	3.34	33.08	18.53	110.52	66.5	90.30
	3–5	0.08	1.98	22.57	3.81	24.14	15.52	18.96	7.7	12.63
	5–10	0.03	1.82	22.04	3.90	21.18	16.05	13.04	3.4	5.99
8 (middle)	0–1	0.06	4.32	18.47	2.53	61.51	11.64	82.87	50.0	18.68
	1–3	0.02	2.77	16.69	1.62	35.04	8.55	10.32	7.6	8.99
	3–5	0.03	3.10	21.38	1.91	37.39	10.54	21.85	13.1	11.36
	5–10	0.02	3.08	14.77	2.06	46.78	11.19	7.97	3.7	6.18
8 (outlet)	0–1	0.20	1.43	11.18	1.69	21.72	10.40	96.51	25.9	27.86
	1–3	0.34	1.11	7.95	1.50	12.07	9.06	39.24	9.0	12.07
	3–5	0.05	1.42	9.52	2.12	14.05	11.51	22.16	4.6	7.12
	5–10	0.02	1.49	16.62	1.92	13.45	11.20	12.55	10.3	4.94